

Self-imaging technique for beam collimation

Luis Miguel Sanchez-Brea,^{1,*} Francisco Jose Torcal-Milla,¹ Jose Maria Herrera-Fernandez,¹ Tomas Morlanes,² and Eusebio Bernabeu¹

¹Optics Department, Applied Optics Complutense Group, Universidad Complutense de Madrid, Facultad de Ciencias Físicas, Ciudad Universitaria s.n., 28040, Madrid, Spain

²AOTEK, Barrio de San Andrés, s.n., 20500, Mondragón, Guipúzcoa, Spain

*Corresponding author: sanchezbrea@fis.ucm.es

Received July 30, 2014; accepted August 31, 2014;
 posted September 4, 2014 (Doc. ID 220041); published 0 MONTH 0000

A simple collimation technique based on measuring the period of one self-image produced by a diffraction grating is proposed. Transversal displacement of the grating is not required, and then automatic single-frame processing can be performed. The self-image is acquired with a CMOS camera, and the period is computed using the variogram function. Analytical and experimental results are obtained, which show the simplicity and accuracy of the proposed technique. © 2014 Optical Society of America

OCIS codes: (050.1940) Diffraction; (050.1950) Diffraction gratings; (070.6760) Talbot and self-imaging effects; (120.1680) Collimation.

<http://dx.doi.org/10.1364/OL.99.099999>

Optical beams with high collimation degree are required in numerous optical applications such as metrology and information processing systems. The simplest technique is auto-collimation, where the size of the beam is compared at two different distances from the source. Nevertheless, more accurate collimation techniques based on self-imaging and interferometry have been developed to obtain a greater collimation degree [1–8]. In addition, dynamic detection method using moiré fringes and grating transverse displacement is proposed in [9,10]. On the other hand, a technique based on double-grating imaging is shown in [11]. In this technique, the optical beam with wavelength λ passes through a diffraction grating with period p . A mask composed by two gratings with the same period p and displaced laterally a distance $p/4$ between them is located at a Talbot plane. Two photodetectors are placed just behind each grating. When the beam is collimated, both signals are shifted 90° , and the Lissajous figure results a circle (considering equal amplitude). When the beam is not collimated, the phase shift between the signals is not exactly 90° , and the Lissajous figure becomes an ellipse. The collimation degree can be determined automatically by measuring the phase shift between both signals.

This technique has been proven robust and accurate. However, a continuous transversal displacement of the grating is required in order to obtain the Lissajous figure. Another technique for beam collimation has been proposed recently, where transversal displacement is not necessary [12]. In this case parabolic fringes are obtained that inform us about the collimation degree by using two gratings, one circular and another linear. Nevertheless the numerical analysis of the fringes to determine the collimation degree is neither simple nor clear.

In this work, we propose a simple and accurate collimation technique based on the self-imaging phenomenon which only requires a diffraction grating and a linear array of photodetectors. Transversal displacement of the grating is not required, and then automatic single-frame processing can be performed. The collimation of the beam is achieved by comparing the period of one self-image with that of the grating until both periods are

equal. We can collimate accurately small-size light beams with this method, provided that Talbot self-images are obtained. In addition, this collimation technique can also be performed for polychromatic light sources, since an achromatic self-imaging regime is also possible [13].

Let us consider the setup shown in Fig. 1. It consists of a point source of wavelength λ , a lens of focal length f , a diffraction grating G , and a CMOS camera. The diffraction grating with period p is placed at a distance z_1 from the lens. The transmittance of the grating is $t(x) = \sum_n a_n \exp(iqn x)$ being n integer numbers, a_n are the Fourier coefficients of the grating, and $q = 2\pi/p$. For amplitude gratings, fringes of the same period as the grating period with maximum contrast are observed at distances $z_2 = lz_T$, where $z_T = 2p^2/\lambda$ is the Talbot distance, and l is an integer. When the emitter is exactly placed at the focal point, $\Delta z = |z_0 - f| = 0$, the beam after the lens is properly collimated, and the period of the self-images is equal to that of the grating. When the emitter is not exactly at the focal point, $\Delta z \neq 0$, the intensity distribution at z_2 results in [11]

$$I(x_3, z_2) \propto I_0 \sum_{n,n'} a_n a_{n'} e^{i \frac{q}{1+\alpha z_2} (n-n') x_3} e^{-i \frac{q^2}{2k} (n^2 - n'^2) \frac{z_2}{1+\alpha z_2}}, \quad (1)$$

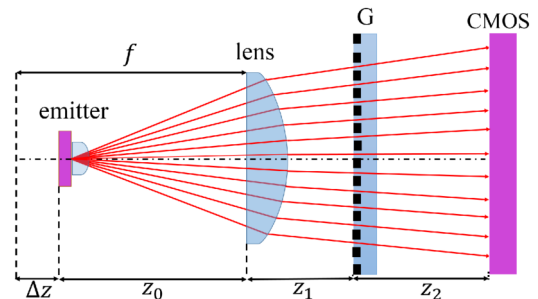


Fig. 1. Experimental setup for beam collimation. z_0 is the distance from emitter to the lens, whose focal length is f , z_1 is the distance from the lens to the diffraction grating G , $\Delta z = z_0 - f$ is the distance from the emitter to the focal point of the lens, and z_2 is the distance from the grating to the observation plane, where a CMOS camera is placed.

80 where x_3 is the coordinate parallel to the grating and
 81 perpendicular to the fringes, I_0 is the intensity of the in-
 82 coming beam, $k = 2\pi/\lambda$, and $\alpha \approx -\Delta z/f^2$. The period of the
 83 fringes $p_{\Delta z}$ is obtained from the first exponential
 84 term,

$$p_{\Delta z} = (1 + \alpha z_2)p. \quad (2)$$

85 where it depends on the distance Δz from the source to
 86 the focal point. On the other hand, the second exponen-
 87 tial term indicates the location of the self images,

$$z_{T,\Delta z} = (1 + \alpha z_2)z_T, \quad (3)$$

88 which are slightly separated when the beam is not
 89 collimated.

90 To measure the collimation of the beam, the best
 91 option is (2) since it is only required the intensity distri-
 92 bution at Talbot distance. Reorganizing Eq. (2) Δz results
 93 in

$$\Delta z = -\frac{f^2}{z_2 p} \Delta p, \quad (4)$$

94 where $\Delta p = p_{\Delta z} - p$ is the variation of the self-image
 95 period with respect to that of the grating. For a certain
 96 set-up, the focal distance of the lens f , the period of the
 97 grating p , and the distance from the grating to the obser-
 98 vation point z_2 are fixed, and the only parameter that
 99 varies with the collimation of the beam is the period
 100 of the fringes at the observation plane $p_{\Delta z}$.

101 For the experimental set-up depicted in Fig. 1, we have
 102 used a diffraction grating with period $p = 100 \mu\text{m}$. The
 103 manufacturing error of the grating is $3 \mu\text{m}/\text{m}$, which cor-
 104 responds to $0.3 \text{ nm}/\text{period}$. The laser diode is HE8807SG
 105 by Hitachi with wavelength $\lambda = 880 \text{ nm}$, and collimation
 106 is performed along the axis perpendicular to the fringes
 107 of the grating. We use a collimation lens with focal
 108 length $f = 25 \text{ mm}$ and diameter $D = 20 \text{ mm}$. Self-images
 109 are acquired with a bidimensional CMOS camera
 110 DMK72BUC02 by Imaging Source whose pixel size is
 111 $2.2 \mu\text{m}$. We have only used one row of the camera,
 112 and for a final set-up, a linear array of photodetectors
 113 can be a simpler option. The CMOS camera is placed
 114 at a distance $z_2 = z_T = 22.7 \text{ mm}$ from the grating. The
 115 grating and the CCD camera have been carefully aligned
 116 to the optical axis. All elements are fixed except the laser
 117 diode, which is displaced along the optical axis with a
 118 step by step motorized stage.

119 The self-images obtained for several positions of the
 120 laser diode are shown in Fig. 2. The step in the displace-
 121 ment is 100 nm . We can see how the period of the fringes
 122 increases, and the intensity of the signal decreases when
 123 the laser diode position Δz is varied. As an example, a
 124 zoom of the self-image profile for $\Delta z + c = 7.5 \text{ mm}$ is
 125 shown in Fig. 3(a). Due to experimental conditions the
 126 self-images are not perfectly uniform and present random
 127 irregularities. These irregularities complicate a proper
 128 period estimation. As a consequence, we have used
 129 the variogram function defined as [14]

$$2\gamma(h) = \langle [I(x+h) - I(x)]^2 \rangle_x, \quad (5)$$

130 where h is the distance between any two data of the
 131 signal, and $\langle \bullet \rangle_x$ means averaging with respect to x , to

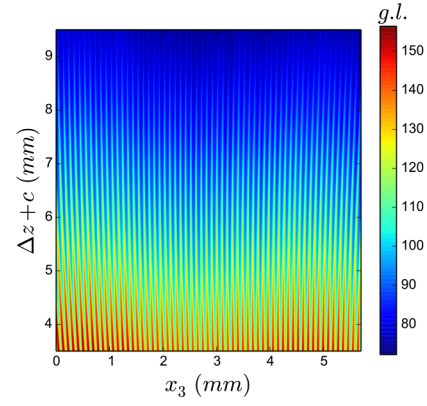


Fig. 2. Experimental fringes for different locations of the laser diode along to the z -axis (grating period $p = 100 \mu\text{m}$ and laser diode wavelength $\lambda = 880 \text{ nm}$). c represents a constant value given by the initial position of the linear stage, which is unknown.

132 filter random fluctuations in the signal. The variogram
 133 function has been used previously for fringe quality
 134 improvement [15,16]. Since each datum of the variogram
 135 is obtained by an averaging, it is much smoother than the
 136 original signal. In addition, the variogram of a periodic
 137 signal is also periodic with the same period. As an exam-
 138 ple, the variogram for the profile of Fig. 3(a) is shown in
 139 Fig. 3(b). Therefore, we can determine the period of the
 140 signal by measuring the period of the variogram, with the
 141 advantage of eliminating random fluctuations and
 142 noise. When the signal is sinusoidal, $I(x) = A + B$
 143 $\sin(qx + \delta)$, the variogram function results in $2\gamma(h) =$
 144 $2B^2 \sin^2(qh/2) = B^2[1 - \cos(qh)]$, where B is the ampli-
 145 tude of the signal. Due to signal irregularities, the
 146 experimental variogram is better fitted to

$$2\gamma(h) = (\alpha + \beta x) - (\gamma + \varepsilon x) \cos(2\pi h/p), \quad (6)$$

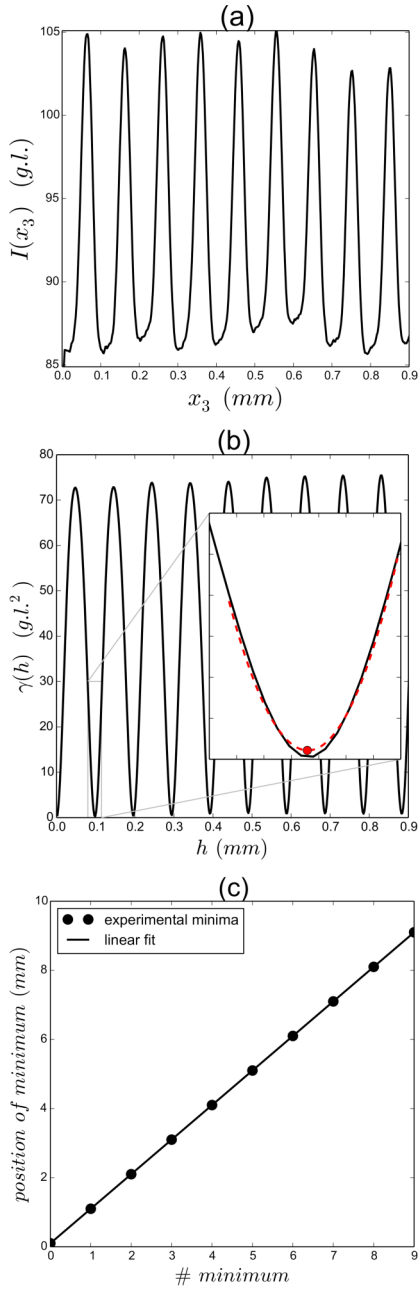
147 where $\alpha, \beta, \gamma, \varepsilon$, and p are free parameters. The param-
 148 eters α, β, γ , and ε can be easily measured from the ex-
 149 perimental variogram. In a first attempt, we have used
 150 the `scipy.optimize` toolbox in Python (www.scipy.org)
 151 in order to obtain the period of the signal for each dis-
 152 tance Δz . The method that has produced best results
 153 is the `minimize_scalar` function [17], where we obtained
 154 a standard deviation of 1.5 nm in the period estimation.
 155 Nevertheless, this technique is quite time consuming, ap-
 156 proximately 6 s for each profile in a Intel Core i7 proc-
 157 essor. As a consequence, for a real-time collimation
 158 technique, we have opted for measuring the location
 159 of the variogram minima by means of a quadratic fitting,
 160 since they are quite parabolic [Fig. 3(b)]. In the example,
 161 we have computed the position for each minimum up to
 162 the ninth, and then we have performed a linear fitting
 163 $y = pn$, where n is the order of the minimum, Fig. 3(c).
 164 The period is obtained as the slope of the fitting. The
 165 processing time for the period estimation was 0.6 s , 10
 166 times faster.

167 The difference $\Delta p = p_{\Delta z} - p$ between the experimen-
 168 tal period $p_{\Delta z}$, obtained for each distance Δz with this
 169 linear fitting, and the period of the grating p is shown in
 170 Fig. 4 (red line). It has been performed for 300 measure-
 171 ments along $30 \mu\text{m}$ of displacement. The histogram of the

F2:1
 F2:2
 F2:3
 F2:4
 F2:5

132
 133
 134
 135
 136
 137
 138
 139
 140
 141
 142
 143
 144
 145
 146

147
 148
 149
 150
 151
 152
 153
 154
 155
 156
 157
 158
 159
 160
 161
 162
 163
 164
 165
 166
 167
 168
 169
 170
 171



F3:1 Fig. 3. (a) Section of the self-image profile of Fig. 2 for
 F3:2 $\Delta z + c = 7.5$ mm. (b) Semi-variogram computed with this signal.
 F3:3 The variogram minima are fitted to a parabolic profile
 F3:4 (dashed line in zoom). Each minimum in the parabolic fitting
 F3:5 (red dot) is used in Fig. 3(c) for period estimation. (c) Linear
 F3:6 fitting of the variogram minima. The computed period is the
 F3:7 slope of the fitting.

172 residuals, $r = \Delta p - (a\Delta z)$, presents a standard deviation
 173 $\delta p = \text{std}(r) = 0.56$ nm, and it is shown in Fig. 5(a). This
 174 standard deviation is comparable to the fluctuations of
 175 period of the grating due to manufacturing errors (ap-
 176 proximately 0.3 nm/period). With this simple algorithm,
 177 we obtain even a better result than when all the
 178 variogram profile is fitted to (6), with minimize_scalar
 179 function (1.5 nm).

180 Finally, we have determined the standard deviation of
 181 the residuals in terms of the number of variogram minima
 182 considered in the linear fitting, Fig. 3(c). In Fig. 5(c), the

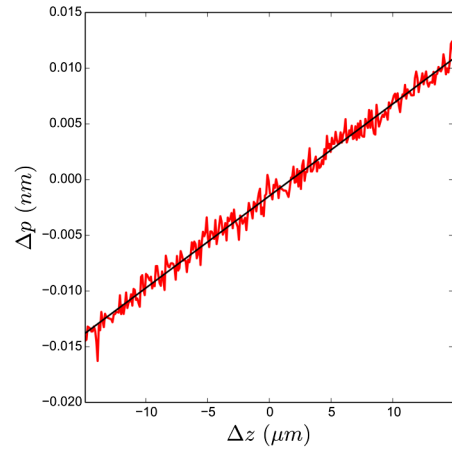


Fig. 4. Difference between the period of the self-image with
 F4:1 respect to that of the grating, Δp , in terms of Δz when the first
 F4:2 10 variogram minima have been used for period estimation (red line).
 F4:3 Linear fitting to these data $\Delta p = a\Delta z$, where $a = 0.00083$
 F4:4 (black line).
 F4:5

standard deviation of the residuals is shown, which de-
 183 creases approximately as $1/N$ by increasing the number
 184 of variogram minima considered in the linear fitting. On
 185 the other hand, when the number of variogram minima is
 186 reduced the algorithm is faster. For example, for $N = 4$
 187 the computation time is 0.16 s, and for $N = 2$ it is only
 188 0.05 s. For this last case, δp is similar to that obtained
 189 with minimize_scalar function (1.5 nm) and 120 times
 190 faster.
 191

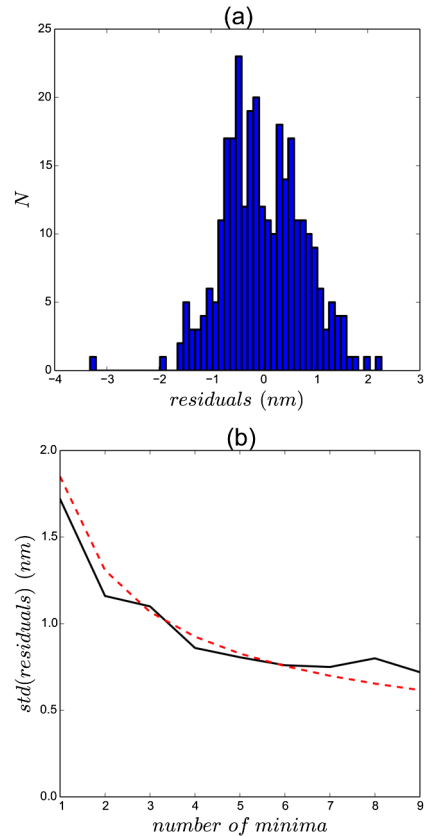


Fig. 5. (a) Histogram of residuals for data of Fig. 4 when 10
 F5:1 variogram minima are used for the period estimation. (b) Stan-
 F5:2 dard deviation of residuals in terms of the number of variogram
 F5:3 minima considered for linear fitting.
 F5:4

192 Finally, since the relationship between position and
 193 period is linear, we can easily determine the resolution
 194 in the divergence of the collimated beam. The resolution
 195 in the location of the emitter results $\delta z = \delta p/a =$
 196 $0.67 \mu\text{m}$, where a is the slope of Fig. 4. These results
 197 are similar to other recent techniques [18–20], with
 198 the advantage of a simpler experimental realization.
 199 Considering the lens equation, $1/s' - 1/s = 1/f'$, with
 200 $s = -f + \delta z$, we obtain that the minimum observable
 201 beam divergence is $\delta\phi = D/2s' \approx D\delta z/2f'^2$. Since we
 202 have used a doublet lens with diameter $D = 20 \text{ mm}$
 203 and focal length $f = 25 \text{ mm}$, the resolution in the diver-
 204 gence of the light beam results $\delta\phi = 10 \mu\text{rad} \approx 0.0006^\circ$.

205 In conclusion, we propose a simple technique for beam
 206 collimation that only uses one diffraction grating and one
 207 linear array of photodetectors. No lateral displacement of
 208 the grating is required. In addition processing of the
 209 signal is very simple since we only have to compute
 210 the period of the self-image captured with the photo-
 211 detector. To reduce the irregularities of the self-image
 212 fringes, we have used the variogram function. Instead
 213 of using an optimization algorithm for the period compu-
 214 tation, we have performed a parabolic fitting of the vario-
 215 gram minima. As a consequence, we have reduced the
 216 computation time up to two orders of magnitude. With
 217 the proposed algorithm we have obtained an experimen-
 218 tal divergence of $10 \mu\text{rad}$ for a doublet lens with diameter
 219 $D = 20 \text{ mm}$ and focal length $f = 25 \text{ mm}$.

220 The authors thank to Jose Luis Vilas for his valuable
 221 comments. This work has been supported by the Ministry
 222 of Science and Innovation of Spain (project DPI2011-
 223 27851) and project Art. 83 LOU “Estudio de tecnología
 224 para la realización de codificadores ópticos de $2 \mu\text{m}$
 225 de periodo” with Fagor Automation S. Coop.

References

1. M. V. R. K. Murthy, *Appl. Opt.* **3**, 531 (1964).
2. D. Malacara, *Optical Shop Testing*, Chap. 4 (Wiley, 1978).
3. A. R. Ganesan and P. Venkateswarlu, *Appl. Opt.* **32**, 2918 (1993).
4. D. E. Silva, *Appl. Opt.* **10**, 1980 (1971).
5. D. Joyeux and Y. Cohen-Sabban, *Appl. Opt.* **21**, 625 (1982).
6. J. Choi, G. Perera, M. Aggarwal, R. Shukla, and M. Mantravadi, *Appl. Opt.* **34**, 3628 (1995).
7. J. S. Darlin, M. P. Kothiyal, and R. S. Sirohi, *J. Mod. Opt.* **45**, 2371 (1998).
8. P. Senthilkumaran, *Appl. Opt.* **42**, 6314 (2003).
9. S. Yokozeki, K. Patorski, and K. Ohnishi, *Opt. Commun.* **14**, 401 (1975).
10. S. Haramaki, S. Yokozeki, A. Hayashi, and H. Suzuki, *Proc. SPIE* **4416**, 388 (2001).
11. L. M. Sanchez-Brea, F. J. Torcal-Milla, F. J. Salgado-Remacha, T. Morlanes, I. Jimenez-Castillo, and E. Bernabeu, *Appl. Opt.* **49**, 3363 (2010).
12. K. Patorski, K. Pokorski, and M. Trusiak, *Opt. Lett.* **39**, 291 (2014).
13. N. Guerineau, B. Harchaoui, and J. Primot, *Opt. Commun.* **180**, 199 (2000).
14. N. Cressie, *Statistics for Spatial Data, revised ed.*, vol. **928** (Wiley, 1993).
15. L. M. Sanchez-Brea, F. J. Torcal-Milla, and E. Bernabeu, *Appl. Opt.* **46**, 5027 (2007).
16. L. M. Sanchez-Brea and E. Bernabeu, *Appl. Opt.* **44**, 3276 (2005).
17. http://docs.scipy.org/doc/scipy/reference/generated/scipy.optimize.minimize_scalar.html.
18. J. Dhanotia and S. Prakash, *Appl. Opt.* **50**, 1446 (2011).
19. R. Disawal, J. Dhanotia, and S. Prakash, *Prec. Eng.* **1** (in press).
20. W. Y. Chang, K. Y. Hsu, K. H. Chen, and J. H. Chen, *Opt. Lasers Eng.* **62**, 126 (2014).

226
227
228
229
230
231
232
233
234
235
236
237
238
239
240
241
242
243
244
245
246
247
248
249
250
251
252
253
254
255
256
257
258
259
260
261
262

Queries

1. AU: Please provide a status update for Ref. [19] if available